Bouncing inflation in a nonlinear R2+R4 gravitational model

PHYSICAL REVIEW D **81,** 124002 (2010)

Bouncing inflation in a nonlinear $R^2 + R^4$ gravitational model

Tamerlan Saidov* and Alexander Zhuk†

Astronomical Observatory and Department of Theoretical Physics, Odessa National University, 2 Dvoryanskaya Street, Odessa 65082, Ukraine

(Received 23 February 2010; published 1 June 2010)

We study a gravitational model with curvature-squared R^2 and curvature-quartic R^4 nonlinearities. The effective scalar degree of freedom ϕ (the scalaron) has a multivalued potential $U(\phi)$ consisting of a number of branches. These branches are fitted with each other in the branching and monotonic points. In the case of four-dimensional space-time, we show that the monotonic points are penetrable for the scalaron, while in the vicinity of the branching points, the scalaron has the bouncing behavior and cannot cross these points. Moreover, there are branching points where the scalaron bounces an infinite number of times with decreasing amplitude, and the Universe asymptotically approaches the de Sitter stage. Such accelerating behavior we call bouncing inflation. For this accelerating expansion, there is no need for original potential $U(\phi)$ to have a minimum or to check the slow-roll conditions. A necessary condition for such inflation is the existence of the branching points. This is a new type of inflation. We show that bouncing inflation takes place both in the Einstein and Brans-Dicke frames.

DOI: 10.1103/PhysRevD.81.124002 PACS numbers: 04.50.Kd, 95.36.+x, 98.80.−k

I. INTRODUCTION

Starting from the pioneering paper [1], the nonlinear (with respect to the scalar curvature R) theories of gravity $f(R)$ have attracted the great deal of interest because these models can provide a natural mechanism of the early inflation. Nonlinear models may arise either due to quantum fluctuations of matter fields including gravity [2], or as a result of compactification of extra spatial dimensions [3]. Compared, e.g., to others higher-order gravity theories, $f(R)$ theories are free of ghosts and of Ostrogradski instabilities [4]. Recently, it was realized that these models can also explain the late-time acceleration of the Universe. This fact resulted in a new wave of papers devoted to this topic (see, e.g., recent reviews [5,6]).

The most simple, and, consequently, the most studied models are polynomials of R: $f(R) = \sum_{n=0}^{k} C_n R^n$ $(k > 1)$, e.g., quadratic $R + R^2$ and quartic $R + R^4$ ones. Active investigation of these models, which started in the 1980s [7,8], continues up to now [9]. Obviously, the correction terms (to the Einstein action) with $n > 1$ give the main contribution in the case of large R, e.g., in the early stages of the Universe's evolution. As it was shown first in [1] for the quadratic model, such modification of gravity results in early inflation. On the other hand, function $f(R)$ may also contain negative degrees of R. For example, the simplest model is $R + R^{-1}$. In this case the correction term plays the main role for small R, e.g., at the late stage of the Universe's evolution (see, e.g., [10,11], and numerous references therein). Such modification of gravity may result in the late-time acceleration of our Universe [12]. Nonlinear models with polynomial as well as R^{-1}-type correction terms have also been generalized to the multidimensional case (see, e.g., [10,11,13–18]).

It is well known that nonlinear models are equivalent to linear-curvature models with additional scalar field ϕ (dubbed the scalaron in [1]). This scalar field corresponds to additional degree of freedom of nonlinear models. The dynamics of this field (as well as a possibility of inflation of the Universe) is defined by potential $U(R(\phi), \phi)$ [see Eq. (2.6) below[1]], where $R = R(\phi)$ is a solution of Eq. (2.3): $\exp(A\phi) = df/dR$. Usually, models or particular cases of these models are considered where this equation has only one solution. In this case, potential U is a one-valued function of ϕ. However, in the most general case this equation has more than one solution and potential becomes a multivalued function with a number of branching points (see, e.g., [19]). Investigation of the dynamical behavior of scalar field and the Universe in such models (especially in the vicinity of the branching points) is not a trivial problem and may result in new important effects. Therefore, it is of interest to consider the models with multivalued potentials.

In the present paper, we study an example of such models. Here, $f(R)$ has both quadratic R^2 and quartic R^4 contributions. In this case Eq. (2.3) is a cubic equation with respect to R and may have, in general, three real solutions/branches $R_i(\phi)$ $(i = 1, 2, 3)$. We have investigated this model in our paper [16]. However, in this paper we considered a special case of one real solution in $D = 8$ space-time. Now, we study the most interesting case of three real solutions. These solutions are fitted with each other in the branching points. There is also another type of matching points where one-valued solutions are fitted with the three-

*tamerlan-saidov@yandex.ru
†ai_zhuk2@rambler.ru

[1]Starting from Sec. II, we denote the scalar curvature of the original nonlinear model by $\bar{R}$.

valued solutions. In the vicinity of these points potential $U(\phi)$ is a monotonic function. Thus, these latter points are dubbed monotonic ones. The main aim of the paper consists in the investigation of dynamical behavior of the system in four-dimensional space-time in the vicinity of the branching and monotonic points. We show that dynamics is quite different for branching and monotonic points. The monotonic points are penetrable for the scalaron, while in the branching points the scalaron has bouncing behavior. There are branching points where the scalaron bounces an infinite number of times with decreasing amplitude and the Universe asymptotically approaches the de Sitter stage. Such accelerating behavior we call *bouncing inflation*. We should note that for this type of inflation, there is no need for original potential $U(\phi)$ to have a minimum or to check the slow-roll conditions. A necessary condition for such inflation is the existence of the branching points. This is a new type of inflation. We show that this inflation takes place both in the Einstein and Brans-Dicke frames. This is the main result of our paper. We think that the scalaron field and the Universe have similar behavior in the vicinity of the branching points for others polynomial and R^{-1}-type models resulting in both early inflation and late-time acceleration. Of course, it is necessary to conduct additional studies of these models, to confirm or refute this assertion.

The paper is structured as follows. In Sec. II we study briefly the equivalence between an arbitrary nonlinear $f(\bar{R})$ theory and theory linear in another scalar curvature R but which contains a scalaron field ϕ. In Sec. III we consider a particular example of nonlinear model with curvature-quadratic and curvature-quartic correction terms and obtain solutions/branches $\bar{R}_i(\phi)$. The fitting procedure for these branches is proposed in Sec. IV. The dynamics of the scalaron and the Universe is investigated in Sec. V. Here, we parametrize the scalaron potential in such a way that it becomes a one-valued function. It provides the possibility to study the dynamical behavior of the system in the vicinity of the branching and monotonic points. We show that in the vicinity of the branching point the scalaron field bounces an infinite number of times with decreasing amplitude, and the Universe acquires the accelerating expansion approaching asymptotically to the de Sitter stage. Such accelerating expansion we call bouncing inflation. A brief discussion of the obtained results is presented in the concluding Sec. VI. In the Appendix, we show that bouncing inflation in the vicinity of the branching point takes place also in the Brans-Dicke frame.

II. GENERAL SETUP

It is well known that nonlinear theories

$$S = \frac{1}{2\kappa_D^2}\int_M d^D x\sqrt{|\bar{g}|}f(\bar{R}), \tag{2.1}$$

where $f(\bar{R})$ is an arbitrary smooth function of a scalar curvature $\bar{R} = R[\bar{g}]$ constructed from the D-dimensional metric $\bar{g}_{ab}$ $(a, b = 1, \ldots, D)$, are equivalent to theories which are linear in another scalar curvature R but which contain an additional self-interacting scalar field. According to standard techniques [7,8], the corresponding R-linear theory has the action functional

$$S = \frac{1}{2\kappa_D^2}\int_M d^D x\sqrt{|g|}[R[g] - g^{ab}\phi_{,a}\phi_{,b} - 2U(\phi)], \tag{2.2}$$

where

$$f'(\bar{R}) = \frac{df}{d\bar{R}} := e^{A\phi} > 0, \qquad A := \sqrt{\frac{D-2}{D-1}}, \tag{2.3}$$

and where the self-interaction potential $U(\phi)$ of the scalar field ϕ is given by

$$U(\phi) = \tfrac{1}{2}(f')^{-D/(D-2)}[\bar{R}f' - f] \tag{2.4}$$

$$= \tfrac{1}{2}e^{-B\phi}[\bar{R}(\phi)e^{A\phi} - f(\bar{R}(\phi))], \tag{2.5}$$

$$B := \frac{D}{\sqrt{(D-2)(D-1)}}. \tag{2.6}$$

The metrics g_{ab}, $\bar{g}_{ab}$ and the scalar curvatures R, $\bar{R}$ of the two theories (2.1) and (2.2) are conformally connected by the relations[2]

$$g_{ab} = \Omega^2\bar{g}_{ab} = [f'(\bar{R})]^{2/(D-2)}\bar{g}_{ab} \tag{2.7}$$

and

$$R = (f')^{2/(2-D)}\Big\{\bar{R} + \frac{D-1}{D-2}(f')^{-2}\bar{g}^{ab}\partial_a f'\partial_b f' - 2\frac{D-1}{D-2}(f')^{-1}\bar{\Box}f'\Big\} \tag{2.8}$$

via the scalar field $\phi = \ln[f'(\bar{R})]/A$. This scalar field ϕ, known as the scalaron [1], carries an additional degree of freedom of original nonlinear model.

According to our definition (2.3), we consider the positive branch $f'(\bar{R}) > 0$. Although the negative $f' < 0$ branch can be considered as well (see, e.g., Refs. [8,10,15]). However, negative values of $f'(\bar{R})$ result in negative effective gravitational "constant" $G_{\text{eff}} = \kappa_D^2/f'$. Thus f' should be positive for the graviton to carry positive kinetic energy (see, e.g., [6]).

From action (2.2), we obtain the equation of motion of the scalaron field ϕ:

$$\Box\phi - \frac{\partial U}{\partial\phi} = 0. \tag{2.9}$$

If scalaron potential $U(\phi)$ has a minimum in a point ϕ_0

[2]The metrics g_{ab} and $\bar{g}_{ab}$ represent the Einstein and Brans-Dicke frames, respectively.

$$\left.\frac{dU}{d\phi}\right|_{\phi_0} = \frac{A}{2(D-2)}(f')^{-D/(D-2)}h|_{\phi_0} = 0,$$
$$h := Df - 2\bar{R}f' \Rightarrow h(\phi_0) = 0, \tag{2.10}$$

then we can define the mass squared of the scalaron [10]:

$$m_\phi^2 = \left.\frac{d^2U}{d\phi^2}\right|_{\phi_0} = \left.\frac{1}{2(D-1)f''}\frac{(D-2)f' - 2\bar{R}f''}{(f')^{2/(D-2)}}\right|_{\phi_0}$$
$$= \left.\frac{(D-2)f' - Dff''/f'}{2(D-1)f''(f')^{2/(D-2)}}\right|_{\phi_0} > 0. \tag{2.11}$$

A similar expression for the scalaron mass squared is also given, e.g., in [6]. The only difference consists of an additional conformal prefactor $1/(f')^{2/(D-2)}$ originated from the conformal metric transformation[3] (2.7). Up to this prefactor, the positiveness condition (2.11) of the mass squared coincides with the stability condition of de Sitter space in $f(\bar{R})$ gravity with respect to inhomogeneous and homogeneous perturbations [6,21]. Additionally, to avoid the Dolgov-Kawasaki instability [22] (instability with respect to local perturbations), it is also required that $f''(\bar{R}) \geq 0$ (see also [23]).

For further research, it is useful to introduce a new variable

$$X := e^{A\phi} - 1. \tag{2.12}$$

Then, potential (2.6) and its first derivative read, correspondingly,

$$U(X) = \tfrac{1}{2}(X+1)^{-B/A}[\bar{R}(X+1) - f] \tag{2.13}$$

and

$$\frac{dU}{dX} = -\frac{B}{2A}(X+1)^{(-B/A)-1}[\bar{R}(X+1) - f]$$
$$+ \frac{1}{2}(X+1)^{-B/A}\bar{R}. \tag{2.14}$$

To conclude this section, we would like to recall that in the multidimensional case, to avoid the effective four-dimensional fundamental constant variation, it is necessary to provide the mechanism of the internal spaces stabilization. In these models, the scale factors of the internal spaces play the role of additional scalar fields (geometrical moduli/gravexcitons [24]). To achieve their stabilization, an effective potential should have minima with respect to all scalar fields (gravexcitons and scalaron). Our previous analysis (see, e.g., [25]) shows that for a model of the form (2.2), the stabilization is possible only for the case of negative minimum of the potential $U(\phi)$. However, it is not difficult to realize that it is impossible to freeze out the internal spaces in such an anti-de Sitter universe. Indeed, in these models scalar fields decrease their amplitude of oscillations around a minimum during the stage of expansion of the Universe [due to a friction term in dynamical equation of the form of (5.2) below] until the Universe reaches its maximum. Then, the Universe turns to the stage of contraction and the amplitudes of scalar fields start to increase again. Thus, geometrical moduli are not stabilized in such models. Therefore, in our present paper we do not investigate the problem of the extra dimension stabilization, but we focus our attention on the dynamics of the scalaron field and the Universe in four-dimensional case.

[3]Conformal transformation for mass squared of scalar fields in models with conformally related metrics is discussed in [20].

III. THE $R^2 + R^4$-MODEL

In this section we analyze a model with curvature-quadratic and curvature-quartic correction terms of the type

$$f(\bar{R}) = \bar{R} + \alpha\bar{R}^2 + \gamma\bar{R}^4 - 2\Lambda_D. \tag{3.1}$$

We start our investigation for an arbitrary number of dimensions D, but in the most particular examples we shall put $D = 4$ (unless stated otherwise). First of all, we define the relation between the scalar curvature $\bar{R}$ and the scalaron field ϕ. According to Eq. (2.3), we have

$$f' = e^{A\phi} = 1 + 2\alpha\bar{R} + 4\gamma\bar{R}^3. \tag{3.2}$$

The definition (2.3) $f' = \exp(A\phi)$ clearly indicates that we choose the positive branch $f' > 0$. For our model (3.1), the surfaces $f' = 0$ as functions $\bar{R} = \bar{R}(\alpha, \gamma)$ are given in Fig. 1. As it easily follows from Eq. (3.2), points where all three values $\bar{R}$, γ, and α are positive correspond to the region $f' > 0$. Thus, this picture shows that we have one simply connected region $f' > 0$ and two disconnected regions $f' < 0$.

Equation (3.2) can be rewritten equivalently in the form

$$\bar{R}^3 + \frac{\alpha}{2\gamma}\bar{R} - \frac{1}{4\gamma}X = 0, \tag{3.3}$$

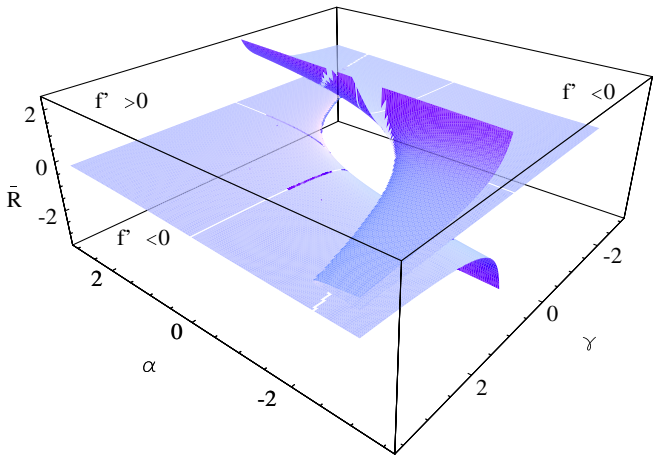

FIG. 1 (color online). The surfaces $f' = 0$ as functions $\bar{R} = \bar{R}(\alpha, \gamma)$ for the model (3.1).

$$X \equiv e^{A\phi} - 1, \qquad -\infty < \phi < +\infty \Rightarrow -1 < X < +\infty. \tag{3.4}$$

Equation (3.3) has three solutions $\bar{R}_{1,2,3}$, where one or three of them are real-valued. Let

$$q := \frac{\alpha}{6\gamma}, \qquad r := \frac{1}{8\gamma} X. \tag{3.5}$$

The sign of the discriminant

$$Q := r^2 + q^3 \tag{3.6}$$

defines the number of real solutions:

$$\begin{aligned} &Q > 0 \Rightarrow \Im \bar{R}_1 = 0, \qquad \Im \bar{R}_{2,3} \neq 0, \\ &Q = 0 \Rightarrow \Im \bar{R}_i = 0 \quad \forall\ i, \qquad \bar{R}_1 = \bar{R}_2, \\ &Q < 0 \Rightarrow \Im \bar{R}_i = 0 \quad \forall\ i. \end{aligned} \tag{3.7}$$

Physical scalar curvatures correspond to real solutions $\bar{R}_i(X)$. It is the most convenient to consider $\bar{R}_i = \bar{R}_i(X)$ as solution family depending on the two additional parameters (α, γ): $\mathrm{sign}(\alpha) = \mathrm{sign}(\gamma) \Rightarrow Q > 0$, $\mathrm{sign}(\alpha) \neq \mathrm{sign}(\gamma) \Rightarrow Q \gtrless 0$. The case $\mathrm{sign}(\alpha) = \mathrm{sign}(\gamma)$ was considered in our paper [16]. In the present paper we investigate the most interesting case $\mathrm{sign}(\alpha) \neq \mathrm{sign}(\gamma)$ of multivalued solutions.

For $Q > 0$, the single real solution $\bar{R}_1$ is given as

$$\bar{R}_1 = [r + Q^{1/2}]^{1/3} + [r - Q^{1/2}]^{1/3} := z_1 + z_2, \tag{3.8}$$

where we can define $z_{1,2}$ in the form

$$z_{1,2}^3 = p e^{\pm\theta}, \qquad p^2 = r^2 - Q = -q^3, \qquad \cosh(\theta) = \frac{r}{\sqrt{-q^3}}. \tag{3.9}$$

Taking into account Eq. (3.5), the function X reads

$$X(\theta) = 8\gamma\sqrt{-q^3}\cosh(\theta). \tag{3.10}$$

The three real solutions $\bar{R}_{1,2,3}(X)$ for $Q < 0$ are given as

$$\begin{aligned} \bar{R}_1 &= s_1 + s_2, \\ \bar{R}_2 &= \tfrac{1}{2}(-1 + i\sqrt{3})s_1 + \tfrac{1}{2}(-1 - i\sqrt{3})s_2 \\ &= e^{i((2\pi)/3)}s_1 + e^{-i((2\pi)/3)}s_2, \\ \bar{R}_3 &= \tfrac{1}{2}(-1 - i\sqrt{3})s_1 + \tfrac{1}{2}(-1 + i\sqrt{3})s_2 \\ &= e^{-i((2\pi)/3)}s_1 + e^{i((2\pi)/3)}s_2, \end{aligned} \tag{3.11}$$

where we can fix the Riemann sheet of $Q^{1/2}$ by setting in the definitions of $s_{1,2}$:

$$s_{1,2} := [r \pm i|Q|^{1/2}]^{1/3}. \tag{3.12}$$

A simple Mathematica calculation gives for Vieta's relations from (3.11)

$$\begin{aligned} \bar{R}_1 + \bar{R}_2 + \bar{R}_3 &= 0, \\ \bar{R}_1\bar{R}_2 + \bar{R}_1\bar{R}_3 + \bar{R}_2\bar{R}_3 &= -3s_1s_2 = 3q, \\ \bar{R}_1\bar{R}_2\bar{R}_3 &= s_1^3 + s_2^3 = 2r. \end{aligned} \tag{3.13}$$

In order to work with explicitly real-valued $\bar{R}_i$, we rewrite $s_{1,2}$ from (3.12) as follows:

$$\begin{aligned} s_{1,2} &= |b|^{1/3}e^{\pm i\vartheta/3}, \\ |b|^2 &= r^2 + |Q| = r^2 - Q = -q^3, \\ \cos(\vartheta) &= \frac{r}{|b|} = \frac{r}{\sqrt{-q^3}}, \end{aligned} \tag{3.14}$$

and get via (3.11)

$$\begin{aligned} \bar{R}_1 &= s_1 + s_2 = 2|b|^{1/3}\cos(\vartheta/3), \\ \bar{R}_2 &= e^{i((2\pi)/3)}s_1 + e^{-i((2\pi)/3)}s_2 \\ &= 2|b|^{1/3}\cos(\vartheta/3 + 2\pi/3), \\ \bar{R}_3 &= e^{-i((2\pi)/3)}s_1 + e^{i((2\pi)/3)}s_2 \\ &= 2|b|^{1/3}\cos(\vartheta/3 - 2\pi/3), \end{aligned} \tag{3.15}$$

or

$$\bar{R}_k = 2|b|^{1/3}\cos\left(\frac{\vartheta + 2\pi k}{3}\right) = 2\sqrt{-q}\cos\left(\frac{\vartheta + 2\pi k}{3}\right), \quad k = -1, 0, 1. \tag{3.16}$$

In order to understand the qualitative behavior of these three real-valued solutions as part of the global solution picture, we first note that, according to (3.3), we may interpret X as single-valued function

$$X(\bar{R}) = 4\gamma\bar{R}^3 + 2\alpha\bar{R} \tag{3.17}$$

and look what is happening when we change (α, γ). Obviously, the inverse function $\bar{R}(X)$ has three real-valued branches when $X(\bar{R})$ is not a monotonic function, but instead has a minimum and a maximum, i.e. when

$$\partial_{\bar{R}}X := X' = 12\gamma\bar{R}^2 + 2\alpha = 0 \Rightarrow \bar{R}^2 = -\frac{\alpha}{6\gamma} \tag{3.18}$$

has two real solutions $\bar{R}_\pm = \pm\sqrt{-\alpha/(6\gamma)}$ and corresponding extrema[4]

$$X(\bar{R}_\pm) = \frac{4}{3}\alpha\bar{R}_\pm. \tag{3.19}$$

It should hold $\mathrm{sign}(\alpha) \neq \mathrm{sign}(\gamma)$ in this case so that we find

$$\begin{aligned} &\gamma > 0, \qquad \alpha < 0\text{: } X_{\max} = X(\bar{R}_-), \qquad X_{\min} = X(\bar{R}_+), \\ &\gamma < 0, \qquad \alpha > 0\text{: } X_{\max} = X(\bar{R}_+), \qquad X_{\min} = X(\bar{R}_-). \end{aligned} \tag{3.20}$$

[4]It is worth of noting that $f''(\bar{R}_\pm) = X'(\bar{R}_\pm) = 0$.

The transition from the three-real-solution regime to the one-real-solution regime occurs when maximum and minimum coalesce at the inflection point

$$\bar{R}_+ = \bar{R}_- = 0 \Rightarrow \alpha = 0, \qquad \gamma \neq 0. \tag{3.21}$$

(We note that here we consider the nondegenerate case $\gamma \neq 0$. Models with $\gamma = 0$ are degenerate ones and are characterized by quadratic scalar curvature terms only.) Because of $-1 \leq X \leq +\infty$, we may consider the limit $X \to +\infty$ where in leading approximation

$$4\gamma\bar{R}^3 \approx X \to +\infty \tag{3.22}$$

so that

$$\bar{R}(X \to \infty) \to \mathrm{sign}(\gamma) \times \infty. \tag{3.23}$$

Leaving the restriction $X \geq -1$ for a moment aside, we have found that for $\alpha\gamma < 0$ there exist three real solution branches $\bar{\mathcal{R}}_{1,2,3}$:

$$\begin{aligned}
\gamma > 0{:}\ & -\infty \leq \bar{\mathcal{R}}_1 \leq \bar{R}_-, && -\infty \leq X \leq X_{\max}, \\
& \bar{R}_- \leq \bar{\mathcal{R}}_2 \leq \bar{R}_+, && X_{\max} \geq X \geq X_{\min}, \\
& \bar{R}_+ \leq \bar{\mathcal{R}}_3 \leq +\infty, && X_{\min} \leq X \leq +\infty, \\
\gamma < 0{:}\ & -\infty \leq \bar{\mathcal{R}}_1 \leq \bar{R}_-, && +\infty \geq X \geq X_{\min}, \\
& \bar{R}_- \leq \bar{\mathcal{R}}_2 \leq \bar{R}_+, && X_{\min} \leq X \leq X_{\max}, \\
& \bar{R}_+ \leq \bar{\mathcal{R}}_3 \leq +\infty, && X_{\max} \geq X \geq -\infty.
\end{aligned} \tag{3.24}$$

It remains for each of these branches to check which of the solutions $\bar{R}_k$ from (3.16) can be fit into this scheme. Finally, one will have to set the additional restriction $X \geq -1$ on the whole picture.

IV. THE FITTING PROCEDURE

We start by considering a concrete example. For definiteness, let us assume $\gamma > 0$, $\alpha < 0$. The pairwise fitting of the various solution branches should be performed at points where $Q = 0$ and different branches of the three-solution sector are fitted with each other or to the branches of the one-solution sector. The points with $Q = 0$ correspond to the X values $X_{\min}$ and $X_{\max}$. Explicitly, we have from (3.19)

$$X(\bar{R}_\pm) = \frac{4}{3}\alpha\bar{R}_\pm = \pm\frac{4}{3}\alpha\sqrt{-\frac{\alpha}{6\gamma}}, \tag{4.1}$$

and for the concrete configuration $\gamma > 0$, $\alpha < 0$

$$\begin{aligned}
X_{\max} &= X(\bar{R}_-) = -\frac{4}{3}\alpha\sqrt{-\frac{\alpha}{6\gamma}} \geq 0, \\
X_{\min} &= X(\bar{R}_+) = \frac{4}{3}\alpha\sqrt{-\frac{\alpha}{6\gamma}} \leq 0.
\end{aligned} \tag{4.2}$$

Next, we find from the defining Eq. (3.14) for the angle ϑ that at $Q = 0$, it holds

$$\cos(\vartheta) = \frac{r}{|b|} = \frac{r}{|r|} \tag{4.3}$$

so that

$$\begin{aligned}
&X_{\max} \geq 0 \Rightarrow r > 0 \Rightarrow \cos(\vartheta) = 1 \Rightarrow \vartheta = 2\pi m, \\
&\quad m \in \mathbb{Z}, \\
&X_{\min} \leq 0 \Rightarrow r < 0 \Rightarrow \cos(\vartheta) = -1 \Rightarrow \vartheta = \pi + 2\pi n, \\
&\quad n \in \mathbb{Z}.
\end{aligned} \tag{4.4}$$

Now, the fitting of the various solution branches can be performed as follows (see Fig. 2). We start with the branch $\Gamma_1 := (R_+ \leq \bar{R} \leq +\infty, X_{\min} < X < +\infty)$. Moving in on this branch from $X \approx +\infty$, we are working in the one-solution sector $Q > 0$ with

$$\bar{R}(\Gamma_1; Q) = [r + Q^{1/2}]^{1/3} + [r - Q^{1/2}]^{1/3} \tag{4.5}$$

until we hit $Q = 0$ at $X = X_{\max}$. At this point $P_1 := (\Gamma_1, X = X_{\max}) \in \Gamma_1$, we have to perform the first fitting. Because of $r > 0$, we may choose

$$\bar{R}(\Gamma_1; Q = 0) = 2r^{1/3} = 2|b|^{1/3} \tag{4.6}$$

so that as simplest parameter choice in (3.16), we set

$$P_1 = (\Gamma_1, X = X_{\max}, Q = 0) \mapsto \vartheta = 0, \qquad k = 0. \tag{4.7}$$

Hence, the parametrization for $(\Gamma_1, Q < 0)$ will be given as

$$\bar{R}(\Gamma_1, Q < 0) = 2|b|^{1/3}\cos(\theta/3). \tag{4.8}$$

For later convenience, we have replaced here the ϑ from Eqs. (3.15) and (3.16) by θ. The reason will become clear from the subsequent discussion. We note that on this Γ_1

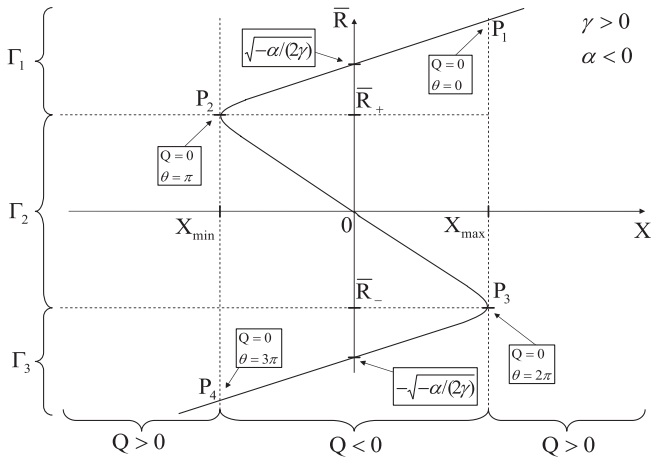

FIG. 2. The schematic drawing of the real solution branches and the matching points $P_{1,2,3,4}$ This figure shows that points $P_{2,3}$ (correspondingly, $\theta = \pi, 2\pi$) and points $P_{1,4}$ (correspondingly, $\theta = 0, 3\pi$) are of a different nature. So, $P_{2,3}$ and $P_{1,4}$ we shall call branching points and monotonic points (in the sense that function $\bar{R}$ is monotonic in the vicinity of these points), respectively.

segment, we may set $\vartheta = \theta$. Let us further move on Γ_1 until its end at $X_{\min}$, where again $Q = 0$. Because there was no other point with $Q = 0$ on this path, the smoothly changing θ can at this local minimum $P_2 = \Gamma_1 \cap \Gamma_2 = (X = X_{\min}, \bar{R} = \bar{R}_+)$ only take one of the values $\theta = \pm\pi$. For definiteness, we choose it as $\theta(P_2) = \pi$. Hence, it holds

$$\bar{R}(P_2) = 2|b|^{1/3}\cos(\pi/3) = |b|^{1/3} = \sqrt{-q} = \sqrt{-\alpha/(6\gamma)} = \bar{R}_+ \tag{4.9}$$

as it should hold. For convenience, we may parametrize our movement on the cubic curve by simply further increasing θ. This gives for moving on $\Gamma_2 = (\bar{R}_+ \geq \bar{R} \geq \bar{R}_-, X_{\min} \leq X \leq X_{\max})$ from the local minimum at P_2 to the local maximum at $P_3 = \Gamma_2 \cap \Gamma_3 = (X = X_{\max}, \bar{R} = \bar{R}_-)$ a further increase of θ by π up to $\theta(P_3) = 2\pi$. Accordingly, we find the complete consistency

$$\bar{R}(P_3) = 2|b|^{1/3}\cos(2\pi/3) = -|b|^{1/3} = -\sqrt{-q} = -\sqrt{-\alpha/(6\gamma)} = \bar{R}_-. \tag{4.10}$$

By further increasing θ up to $\theta = 3\pi$, we reach the point $P_4 = (X = X_{\min}, Q = 0) \in \Gamma_3$ with

$$\bar{R}(P_4) = 2|b|^{1/3}\cos(3\pi/3) = -2|b|^{1/3} = -2|r|^{1/3}. \tag{4.11}$$

Because of $r < 0$, we can smoothly fit it to the one-solution branch

$$\bar{R}(\Gamma_4, Q) = [r + Q^{1/2}]^{1/3} + [r - Q^{1/2}]^{1/3} \tag{4.12}$$

by setting trivially

$$\bar{R}(P_4) = 2(-|r|)^{1/3} = -2|r|^{1/3}. \tag{4.13}$$

Summarizing, we arrived at a very simple and transparent branch fitting picture, where all the movement in the three-solution sector can be parametrized by choosing the effective angle as $\theta \in [0, 3\pi]$. Finally, we have to fit this picture in terms of smoothly varying $\theta \in [0, 3\pi]$ with the three solutions $\bar{R}_k$ from (3.16). For this purpose, we note that the single value $\vartheta \in [0, \pi]$ in (3.16) is a projection of our smoothly varying $\theta \in [0, 3\pi]$. Fixing an arbitrary ϑ, one easily finds the following correspondences:

$$\theta(\Gamma_1, \vartheta) = \vartheta, \qquad \theta(\Gamma_2, \vartheta) = 2\pi - \vartheta, \qquad \theta(\Gamma_3, \vartheta) = 2\pi + \vartheta \tag{4.14}$$

and hence

$$\begin{aligned}
\bar{R}[\theta(\Gamma_1, \vartheta)] &= 2|b|^{1/3}\cos\left(\frac{\vartheta}{3}\right) = \bar{R}_{(k=0)} = \bar{\mathcal{R}}_3,\\
\bar{R}[\theta(\Gamma_2, \vartheta)] &= 2|b|^{1/3}\cos\left(\frac{2\pi - \vartheta}{3}\right)\\
&= 2|b|^{1/3}\cos\left(\frac{\vartheta - 2\pi}{3}\right) = \bar{R}_{(k=-1)} = \bar{\mathcal{R}}_2,\\
\bar{R}[\theta(\Gamma_3, \vartheta)] &= 2|b|^{1/3}\cos\left(\frac{2\pi + \vartheta}{3}\right) = \bar{R}_{(k=1)} = \bar{\mathcal{R}}_1.
\end{aligned} \tag{4.15}$$

Analogically, we can obtain rules for fitting procedure in the case $\gamma < 0$, $\alpha > 0$. So, all the fitting mechanism is clear now and can be used in further considerations.

V. DYNAMICS OF THE UNIVERSE AND SCALARON

To study the dynamics of the Universe in our model, we assume that the four-dimensional metric g in (2.7) is spatially flat Friedmann-Robertson-Walker one:

$$g = -dt \otimes dt + a^2(t)d\vec{x} \otimes d\vec{x}. \tag{5.1}$$

Thus, scalar curvatures R and $\bar{R}$ and the scalaron ϕ are functions of time. Therefore, Eq. (2.9) for homogeneous field ϕ reads

$$\ddot{\phi} + 3H\dot{\phi} + \frac{dU}{d\phi} = 0, \tag{5.2}$$

where the Hubble parameter $H = \dot{a}/a$ and the dots denote the differentiation with respect to time t. Potential U is defined by Eq. (2.6). Because U depends on $\bar{R}$ which is a multivalued function of ϕ (or, equivalently, of X), the potential U is also a multivalued function of X (see Fig. 3).[5] However, our previous analysis shows that we can avoid this problem making X and $\bar{R}$ single-valued functions of a new field θ (we recall that we consider the particular case of $\alpha\gamma < 0$ when $\alpha < 0$, $\gamma > 0$):

$$X(\theta) = \begin{cases} \sqrt{(1/\gamma)(2|\alpha|/3)^3}\cosh(\theta), & \theta < 0;\\ \sqrt{(1/\gamma)(2|\alpha|/3)^3}\cos(\theta), & 0 \leq \theta \leq 3\pi;\\ -\sqrt{(1/\gamma)(2|\alpha|/3)^3}\cosh(\theta - 3\pi), & \theta > 3\pi; \end{cases} \tag{5.3}$$

and

[5] In spite of the divergency of $d\bar{R}/dX$ in the branching points $P_{2,3}$, the derivatives dU/dX are finite in these points in accordance with Eq. (2.14). Moreover, $\bar{R}$ and X have the same values in branching points for different branches. Therefore, the branches arrive at the branching points with the same values of dU/dX, and Fig. 3 clearly shows it.

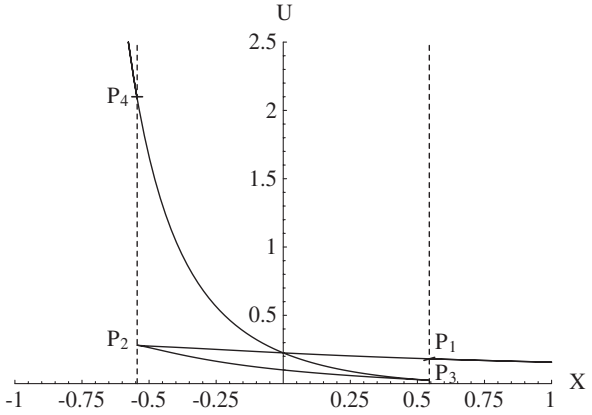

FIG. 3. The form of the potential (2.6) as a multivalued function of $X = e^{A\phi} - 1$ in the case $D = 4$, $\Lambda_4 = 0.1$, $\gamma = 1$, and $\alpha = -1$. Points $P_{1,2,3,4}$ are defined in Fig. 2.

$$\bar{R}(\theta) = \begin{cases} 2\sqrt{|\alpha|/(6\gamma)}\cosh(\theta/3), & \theta < 0; \\ 2\sqrt{|\alpha|/(6\gamma)}\cos(\theta/3), & 0 \le \theta \le 3\pi; \\ -2\sqrt{|\alpha|/(6\gamma)}\cosh[(\theta/3) - \pi], & \theta > 3\pi. \end{cases} \tag{5.4}$$

The function $X = X(\theta)$ is schematically given in Fig. 4. It is necessary to keep in mind that we consider the case $f' > 0 \rightarrow X > -1$. If we demand that $X_{\min} > -1$ (in opposite case our graphic $X(\theta)$ will be cut into two disconnected parts), then the parameters α and γ should satisfy the inequality:

$$X_{\min} = -\sqrt{(1/\gamma)(2|\alpha|/3)^3} > -1 \Rightarrow |\alpha| \le \tfrac{3}{2}\gamma^{1/3}. \tag{5.5}$$

The maximal value of θ (which is greater than 3π in the case $X_{\min} > -1$) is defined from the transcendental equation

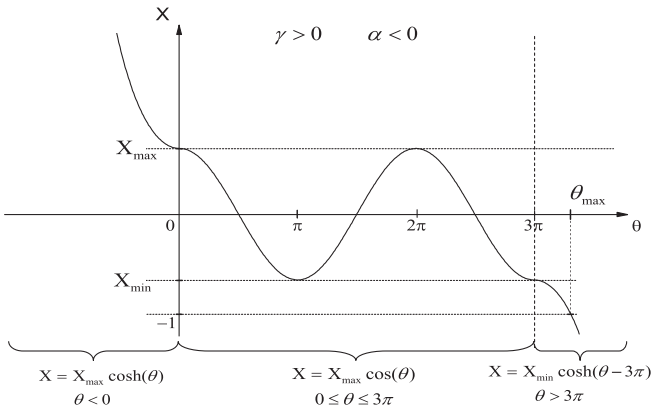

FIG. 4. The schematic drawing of Eq. (5.3) in the case $X_{\min} > -1$. Here, $X_{\max} = \sqrt{(1/\gamma)(2|\alpha|/3)^3}$, $X_{\min} = -\sqrt{(1/\gamma)(2|\alpha|/3)^3}$ and $\theta_{\max}$ is defined by Eq. (5.6).

$$\tfrac{1}{2}[(c + \sqrt{c^2 - 1})^{1/3} + (c - \sqrt{c^2 - 1})^{1/3}] = \cosh[(\theta_{\max}/3) - \pi], \tag{5.6}$$

where $c := (\sqrt{(1/\gamma)(2|\alpha|/3)^3})^{-1}$. The limit $X \rightarrow -1$ corresponds to the limit $\theta \rightarrow \theta_{\max}$. With the help of Eq. (5.3) and formula

$$\frac{d\phi}{d\theta} = \frac{1}{A(X+1)}\frac{dX}{d\theta}, \tag{5.7}$$

we can also get the following useful expressions:

$$\left.\frac{d\phi}{d\theta}\right|_{\theta=0,\pi,2\pi,3\pi} = \left.\frac{dX}{d\theta}\right|_{\theta=0,\pi,2\pi,3\pi} = 0. \tag{5.8}$$

It can be easily verified that field θ satisfies the following equation:

$$\ddot{\theta} + 3H\dot{\theta} + \Gamma(\theta)\dot{\theta}^2 + G(\theta)\frac{dU}{d\theta} = 0. \tag{5.9}$$

Here, we introduce the one dimensional metric on the moduli space $G(\theta) \equiv G^{11} = (G_{11})^{-1} = (d\phi/d\theta)^{-2}$ with the corresponding Christoffel symbol $\Gamma(\theta) \equiv \Gamma^1_{11} = (1/2)G^{11}(G_{11})_{,\theta} = (d^2\phi/d\theta^2)/(d\phi/d\theta)$.

A. Properties of the potential $U(\theta)$

As we mentioned above, the potential (2.6) as a function of θ is a single-valued one. Now, we want to investigate analytically some general properties of $U(\theta)$. In this subsection, D is an arbitrary number of dimensions and signs of α and γ are not fixed if it is not specified particularly.

First, we consider the *extrema of the potential* $U(\theta)$. To find the extremum points, we solve the equation

$$\frac{dU}{d\theta} = \frac{dU}{d\phi}\frac{d\phi}{d\theta} = \frac{dU}{d\phi}\frac{1}{A(X+1)}\frac{dX}{d\theta} = 0. \tag{5.10}$$

Therefore, the extrema correspond either to the solutions of the Eq. (2.10) $dU/d\phi = 0$ for finite $dX/d\theta$ ($X > -1$) or to the solutions of the equation $dX/d\theta = 0$ ($X > -1$) for finite $dU/d\phi$. The form of the potential U [see Eqs. (2.4) and (2.6)] shows that this potential and its derivative $dU/d\phi$ is finite for $X > -1$. Thus, as it follows from Eq. (5.8), the potential $U(\theta)$ has extrema at the matching points $\theta = 0$, π, 2π, 3π. Additional extremum points are real solutions of the Eq. (2.10). For our model (3.1), this equation reads

$$\bar{R}^4\gamma\left(\frac{D}{2} - 4\right) + \bar{R}^2\alpha\left(\frac{D}{2} - 2\right) + \bar{R}\left(\frac{D}{2} - 1\right) - D\Lambda_D = 0. \tag{5.11}$$

The form of this equation shows that there are two particular cases: $D = 8$ and $D = 4$. The $D = 8$ case was considered in [16]. Let us consider now the case $D = 4$:

$$\bar{R}^4 - \frac{1}{2\gamma}\bar{R} + \frac{2\Lambda_4}{\gamma} = 0. \tag{5.12}$$

It is worth of noting that parameter α disappeared from this equation. Thus α has no an influence on a number of additional extremum points. To solve this quartic equation, we should consider an auxiliary cubic equation

$$u^3 - \frac{8\Lambda_4}{\gamma}u - \frac{1}{4\gamma^2} = 0. \tag{5.13}$$

The analysis of this equation can be performed in similar manner as we did it for the cubic Eq. (3.3). Let us introduce the notations:

$$\bar{q} := -\frac{8}{3}\frac{\Lambda_4}{\gamma}, \qquad \bar{r} := \frac{1}{8}\frac{1}{\gamma^2},$$
$$\bar{Q} := \bar{r}^2 + \bar{q}^3 = \frac{1}{\gamma^4}\left(\frac{1}{8^2} - \gamma\left(\frac{8\Lambda_4}{3}\right)^3\right). \tag{5.14}$$

It make sense to consider two separate cases.

1. $\mathrm{sign}\gamma = -\mathrm{sign}\Lambda_4 \Rightarrow \bar{Q} > 0$.

In this case we have only one real solution of Eq. (5.13):

$$u_1 = [\bar{r} + \bar{Q}^{1/2}]^{1/3} + [\bar{r} - \bar{Q}^{1/2}]^{1/3} > 0. \tag{5.15}$$

Then, solutions of the quartic (5.12) are the real roots of two quadratic equations

$$\bar{R}^2 \pm \sqrt{u_1}\bar{R} + \frac{1}{2}(u_1 \pm \epsilon\sqrt{u_1^2 + 3q}) = 0, \qquad \epsilon = \mathrm{sign}\gamma. \tag{5.16}$$

Simple analysis shows that for any sign of γ we obtain two real solutions:

$$\gamma < 0 \Rightarrow \bar{R}^{(+)}_{1,2} = -\tfrac{1}{2}u_1^{1/2} \pm \sqrt{-\tfrac{1}{4}u_1 + \tfrac{1}{2}(u_1^2 + 3q)^{1/2}},$$
$$\gamma > 0 \Rightarrow \bar{R}^{(-)}_{1,2} = \tfrac{1}{2}u_1^{1/2} \pm \sqrt{-\tfrac{1}{4}u_1 + \tfrac{1}{2}(u_1^2 + 3q)^{1/2}}. \tag{5.17}$$

2. $\mathrm{sign}\gamma = \mathrm{sign}\Lambda_4 \Rightarrow \bar{Q} \gtrless 0$.

It is not difficult to show that in this case the real solutions of the form of (5.17) (where we should make the evident substitution $u_1^2 + 3q \to u_1^2 - 3|q|$) takes place if

$$\bar{Q} > 0 \Rightarrow |\gamma|^{1/3} < \frac{3}{32|\Lambda_4|}. \tag{5.18}$$

Now, we want to investigate *zeros of the potential* U. For $f' \neq 0 \Rightarrow X \neq -1$, the condition of zeros of the potential (2.4) is

$$\bar{R}f' - f = 0 \Rightarrow 3\gamma\bar{R}^4 + \alpha\bar{R}^2 + 2\Lambda_D = 0. \tag{5.19}$$

Therefore, zeros are defined by equation

$$\bar{R}^2 = -\frac{\alpha}{6\gamma} \pm \left[\left(\frac{\alpha}{6\gamma}\right)^2 - \frac{2\Lambda_D}{3\gamma}\right]^{1/2}. \tag{5.20}$$

Obviously, the necessary conditions for zeros are

$$\gamma > 0 \Rightarrow \Lambda_D \leq \alpha^2/(24\gamma),$$
$$\gamma < 0 \Rightarrow \Lambda_D \geq -\alpha^2/(24|\gamma|). \tag{5.21}$$

Additionally, we should check that the right-hand side of the Eq. (5.20) is positive.

Let us consider now *asymptotical behavior of the potential* $U(\theta)$. Here, we want to investigate limits $\theta \to \theta_{\max}$ and $\theta \to -\infty$. In the former case we get

$$\theta \to \theta_{\max} \Rightarrow U(\theta) \to -\mathrm{sign}(f(\theta_{\max})) \times \infty. \tag{5.22}$$

In the latter case we obtain

$$\theta \to -\infty \Rightarrow U(\theta) \sim \exp\left(\frac{8-D}{D-2}\theta\right)$$
$$\to \begin{cases} +\infty, & D > 8; \\ \mathrm{const} > 0, & D = 8; \\ +0, & 2 < D < 8; \end{cases} \tag{5.23}$$

where we used Eqs. (5.3) and (5.4). This result coincides with conclusions of Appendix A in [16].

To illustrate the described above properties, we draw the potential $U(\theta)$ in Fig. 5 for the following parameters: $D = 4$, $\Lambda_4 = 0.1$, $\gamma = 1$, and $\alpha = -1$. These parameters contradict the inequalities (5.18) and (5.21). Therefore, $\theta = 0$, π, 2π, 3π are the only extremum points of the potential $U(\theta)$, and zeros are absent. These parameters are also satisfy the condition (5.5). The absence of zeros means that all minima of the potential $U(\theta)$ are positive.

For our subsequent investigations, it is useful also to consider an effective force and mass squared of the field θ. As it follows from Eq. (5.9), the effective force is

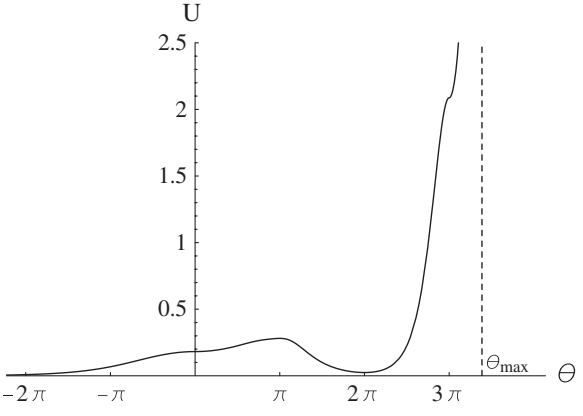

FIG. 5. The form of the potential (2.6) as a function of θ in the case $D = 4$, $\Lambda_4 = 0.1$, $\gamma = 1$, and $\alpha = -1$. For these values of the parameters, all extrema correspond to the matching points $\theta = 0$, π, 2π, 3π. In the branching points $\theta = \pi$, 2π the potential has local maximum and local nonzero minimum, respectively, and the monotonic points $\theta = 0$, 3π are the inflection ones. Potential tends asymptotically to $+\infty$ when θ goes to $\theta_{\max}$ and to zero when $\theta \to -\infty$.

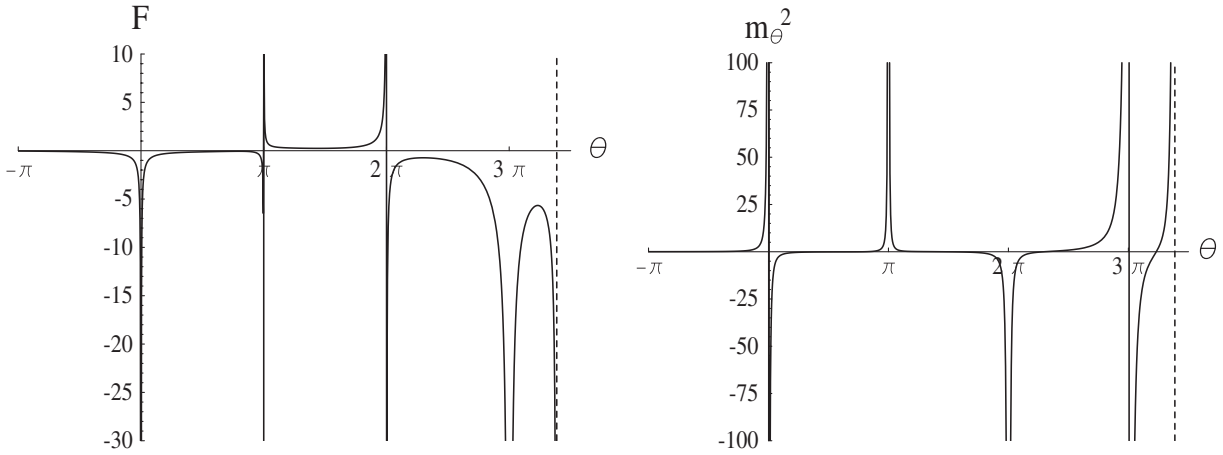

FIG. 6. The effective force (5.24) (left panel) and the mass squared (5.25) (right panel) for the potential $U(\theta)$ drawn in Fig. 5. These pictures clearly show singular behavior of F and m_θ^2 in the matching points $\theta = 0,\ \pi,\ 2\pi,\ 3\pi$.

$$F = -G(\theta)\frac{dU}{d\theta}. \tag{5.24}$$

Varying Eq. (5.9) with respect to field θ, we obtain dynamical equation for small fluctuation $\delta\theta$ where mass squared reads

$$m_\theta^2 = G(\theta)\frac{d^2U}{d\theta^2} + \frac{dG(\theta)}{d\theta}\frac{dU}{d\theta}. \tag{5.25}$$

In Fig. 6 we show the effective force and the mass squared as functions of θ for the potential drawn in Fig. 5. These figures indicate that field θ may have very nontrivial behavior. This nontriviality follows from two reasons. First, the field θ has noncanonical kinetic term which result in appearing of nonflat moduli space metric $G(\theta)$ and derivative of $G(\theta)$ in Eq. (5.9). Second, the function $G(\theta)$ has singular behavior at the matching points $\theta = 0,\ \pi, 2\pi, 3\pi$. Thus, our intuition does not work when we want to predict dynamical behavior of fields with equations of the form of (5.9) with potential drawn in Fig. 5, especially when field approaches the matching points. It is necessary to solve equations analytically or to investigate them numerically. Such analysis for our model is performed in the next subsection where we concentrate our attention to the most interesting case where all extrema correspond to the matching points $\theta = 0,\ \pi,\ 2\pi,\ 3\pi$.

B. Dynamical behavior of the Universe and field θ

Now, we intend to investigate dynamical behavior of scalar field θ and the scale factor a in more detail. There are no analytic solutions for considered model. So, we use numerical calculations. To do it, we apply a Mathematica package proposed in [26] and adjusted to our models and notations in Appendix A of our paper [18]. According to these notations, all dimensional quantities in our graphics are given in the Planck units. Additionally, in the present paper we should remember that metric on the moduli space is not flat and defined in Eq. (5.9). For example, the canonical momenta and the kinetic energy read

$$\begin{aligned} P_\theta &= \frac{a^3}{\kappa_4^2}G_{11}\dot\theta = \frac{a^3}{\kappa_4^2}\left(\frac{d\phi}{d\theta}\right)^2\dot\theta, \\ E_{\rm kin} &= \frac{1}{2\kappa_4^2}G_{11}\dot\theta^2 = \frac{\kappa_4^2}{2a^6}G^{11}P_\theta^2 = \frac{1}{2\kappa_4^2}\left(\frac{d\phi}{d\theta}\right)^2\dot\theta^2, \end{aligned} \tag{5.26}$$

where $8\pi G \equiv \kappa_4^2$ and G is four-dimensional Newton constant. To understand the dynamics of the Universe, we shall also draw the Hubble parameter

$$3\left(\frac{\dot a}{a}\right)^2 \equiv 3H^2 = \frac{1}{2}G_{11}\dot\theta^2 + U(\theta) \tag{5.27}$$

and the acceleration parameter

$$q \equiv \frac{\ddot a}{H^2 a} = \frac{1}{6H^2}\left(-4 \times \frac{1}{2}G_{11}\dot\theta^2 + 2U(\theta)\right). \tag{5.28}$$

Figure 6 shows that the effective force changes its sign and the mass squared preserves the sign when θ crosses the branching points π, 2π and vise versa, the effective force preserves the sign and the mass squared changes the sign when θ crosses the monotonic points 0, 3π. Therefore, it make sense to consider these cases separately.

1. Branching points $\theta = \pi,\ 2\pi$

First, we consider the dynamical behavior of the Universe and a scalaron in the vicinity of the branching point $\theta = 2\pi$ which is the local minimum of the potential in Fig. 5. The time evolution of a scalaron field θ and its kinetic energy $E_{\rm kin}$ are drawn in Fig. 7. Here and in all pictures below, we use the same parameters as in Fig. 5. The time t is measured in the Planck times and classical evolution starts at $t = 1$. For the initial value of θ, we take $\theta_{\rm initial} = 3.5$. We plot in Fig. 8 the evolution of the logarithms of the scale factor $a(t)$ (left panel) and the evolution of the Hubble parameter $H(t)$ (right panel) and in Fig. 9 the

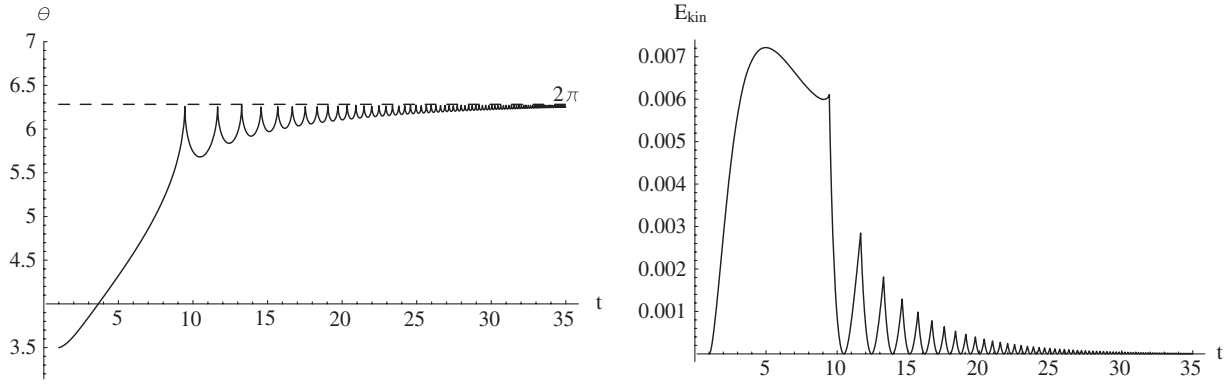

FIG. 7. Dynamical behavior of scalar field $\theta(t)$ (left panel) and its kinetic energy $E_{\rm kin}(t)$ (right panel) in the vicinity of the branching point $\theta = 2\pi$.

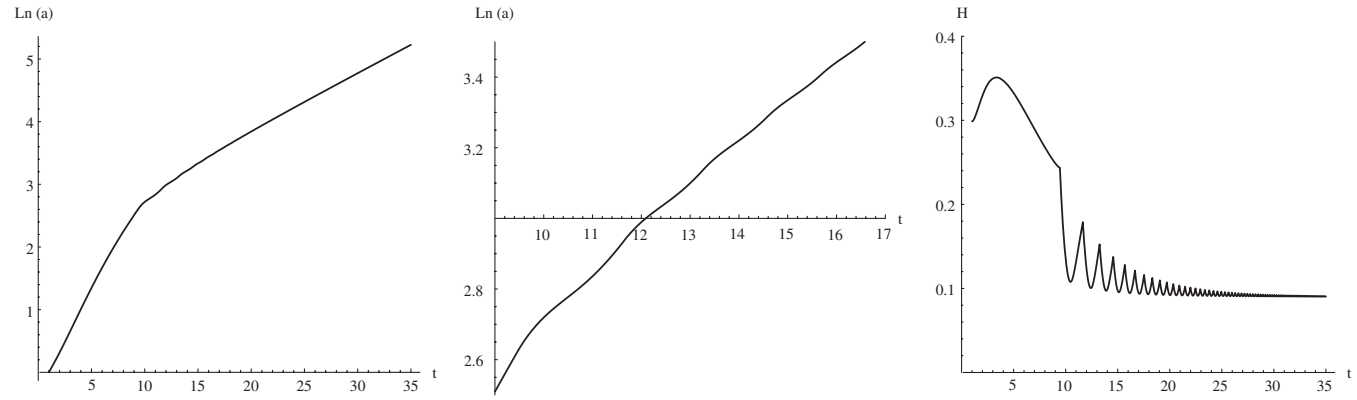

FIG. 8. The time evolution of the logarithms of the scale factor $a(t)$ (left panel) and the Hubble parameter $H(t)$ (right panel) for the trajectory drawn in Fig. 7. A slightly visible oscillations of $\ln(a)$ (caused by bounces) can be seen by magnification of this picture (middle panel).

evolution of the parameter of acceleration $q(t)$ (left panel) and the equation of state parameter $\omega(t) = [2q(t) + 1]/3$ (right panel).

Figure 7 demonstrates that scalar field θ bounces an infinite number of times with decreasing amplitude in the vicinity of the branching point $\theta = 2\pi$. θ cannot cross this point. From Figs. 8 and 9, we see that the Universe asymptotically approaches the de Sitter stage: $H \to$ const, $q \to +1$, and $\omega \to -1$. Such accelerating behavior we call bouncing inflation.

Concerning the dynamical behavior in the vicinity of the branching point $\theta = \pi$, our analysis (similar performed above) shows that the scalaron field θ cannot cross this local maximum regardless of the magnitude of initial velocity in the direction of $\theta = \pi$. It bounces back from this point.

2. *Monotonic points* $\theta = 0, 3\pi$

Now, we want to investigate the dynamical behavior of the model in the vicinity of the monotonic points $\theta = 0$, 3π which are the points of inflection of the potential in Fig. 5. Figures 5 and 6 show that for both of these points the model has the similar dynamical behavior. Therefore, for definiteness, we consider the point $\theta = 3\pi$. To investigate numerically the crossing of the monotonic point 3π, it is necessary to take very small value of a step Δt. It can be achieved if we choose very large value of the maximum number of steps. Thus, for the given value of the maximum number of steps, the closer to 3π the initial value $\theta_{\rm initial}$ is taken, the smaller step Δt we obtain. For our calculation, we choose $\theta_{\rm initial} = 9.513$. Figure 10 demonstrates that scalar field θ slowly crosses the monotonic point 3π with nearly zero kinetic energy.[6] Then, just after the crossing, the kinetic energy has its maximum value and starts to decrees gradually when θ moves to the direction 2π.

Figures 11 and 12 demonstrate the behavior of the Universe before and after crossing 3π. We do not show here the vicinity of the branching point 2π because when θ approaches 2π the Universe has the bouncing inflation described above. Hence, there are 3 phases sequentially:

[6]The derivative $d\theta/dt$ goes to $-\infty$ when $\theta \to 3\pi$ (with different speed on different sides of 3π) but $d\phi/d\theta = 0$ at 3π and kinetic energy is finite [see Eq. (5.26)].

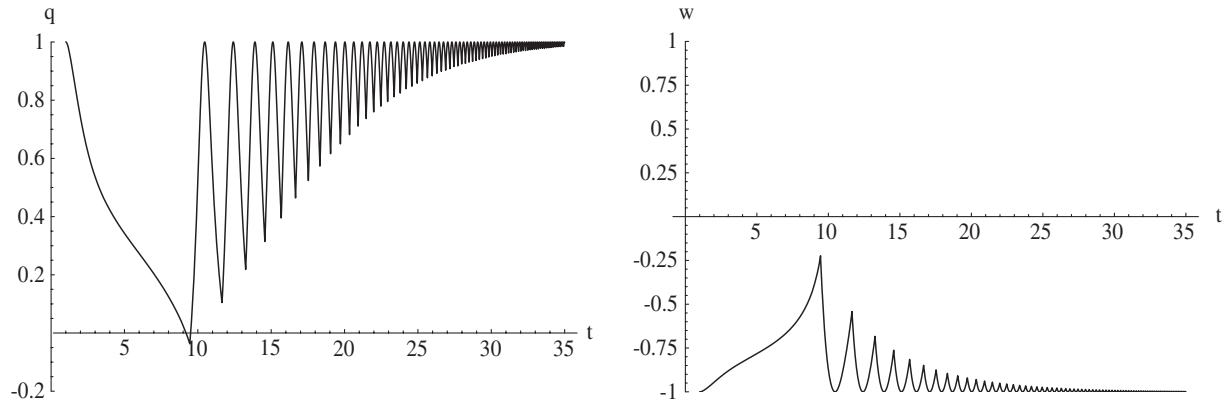

FIG. 9. The parameter of acceleration $q(t)$ (left panel) and the equation of state parameter $\omega(t)$ (right panel) for the scale factor in Fig. 8.

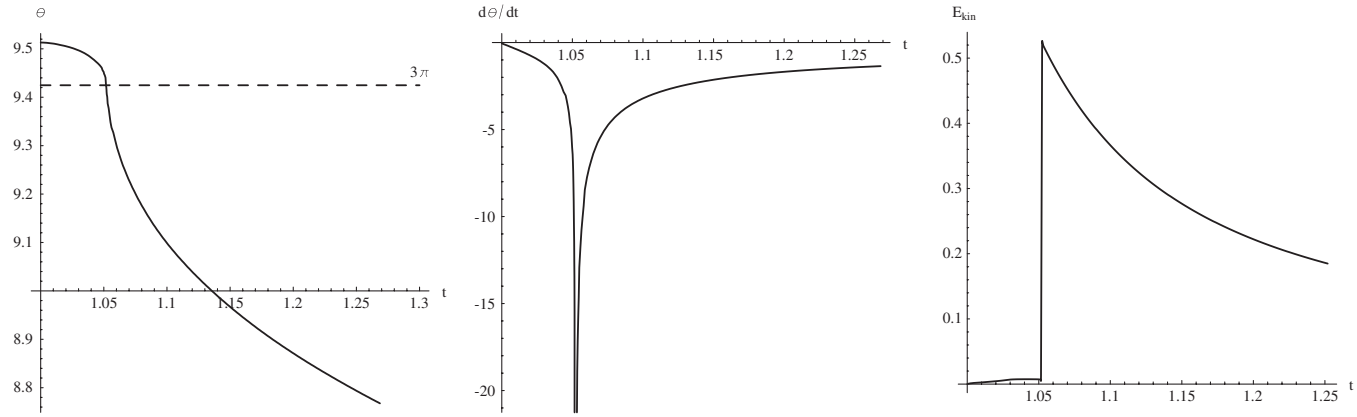

FIG. 10. Dynamical behavior of scalar field $\theta(t)$ (left panel) and its time derivative $d\theta/dt$ (middle panel) and kinetic energy $E_{\rm kin}(t)$ (right panel) for the case of crossing of the inflection point $\theta = 3\pi$.

the short de Sitter-like stage during slow rolling in the vicinity of the inflection point before crossing, then decelerating expansion just after the crossing with gradual transition to the accelerating stage again when θ approaches the branching point 2π. Clearly, for another monotonic point $\theta = 0$, we get the similar crossing behavior (without the bouncing stage when $\theta \to -\infty$). Therefore, the monotonic points $\theta = 0$ and $\theta = 3\pi$ are penetrable for the scalaron field θ.

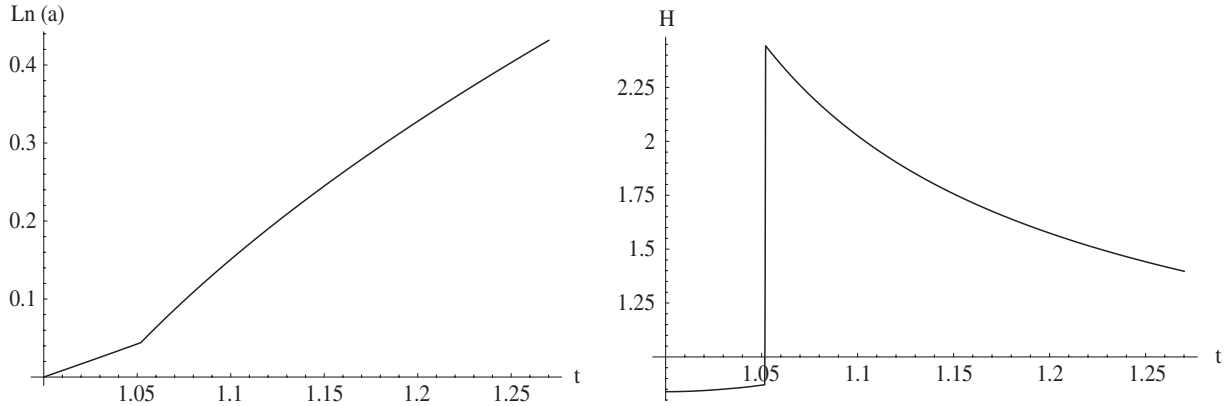

FIG. 11. The time evolution of the logarithms of the scale factor $a(t)$ (left panel) and the Hubble parameter $H(t)$ (right panel) for the trajectory drawn in Fig. 10.

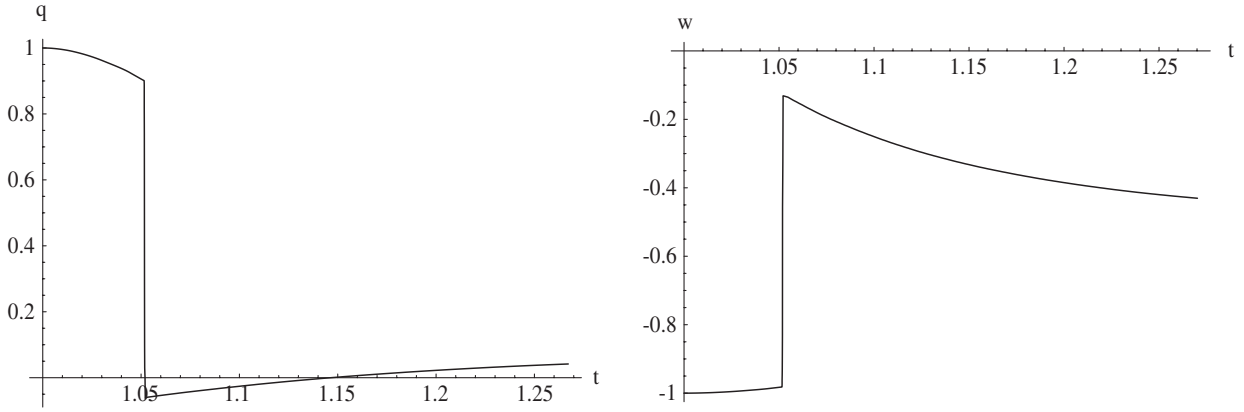

FIG. 12. The parameter of acceleration $q(t)$ (left panel) and the equation of state parameter $\omega(t)$ (right panel) for the scale factor in Fig. 11.

VI. CONCLUSIONS

We have investigated the dynamical behavior of the scalaron field ϕ and the Universe in nonlinear model with curvature-squared and curvature-quartic correction terms: $f(\bar{R}) = \bar{R} + \alpha\bar{R}^2 + \gamma\bar{R}^4 - 2\Lambda_D$. We have chosen parameters α and γ in such a way that the scalaron potential $U(\phi)$ is a multivalued function consisting of a number of branches. These branches are fitted with each other either in the branching points (points $P_{2,3}$ in Fig. 3) or in the monotonic points (points $P_{1,4}$ in Fig. 3). We have reparametrized the potential U in such a way that it becomes the one-valued function of a new field variable $\theta = \theta(\phi)$ (see Fig. 5). This has enabled us to consider the dynamical behavior of the system in the vicinity of the branching and monotonic points in $(D = 4)$-dimensional space-time. Our investigations show that the monotonic points are penetrable for the scalaron field (see Figs. 10–12), and while in the vicinity of the branching points, the scalaron has the bouncing behavior and cannot cross these points. Moreover, there are branching points where the scalaron bounces an infinite number of times with decreasing amplitude and the Universe asymptotically approaches the de Sitter stage (see Figs. 7–9). Such accelerating behavior we call bouncing inflation. It should be noted that for this type of inflation there is no need for original potential $U(\phi)$ to have a minimum or to check the slow-roll conditions. A necessary condition is the existence of the branching points. This is a new type of inflation. We show that this inflation takes place both in the Einstein and Brans-Dicke frames. We have found this type of inflation for the model with the curvature-squared and curvature-quartic correction terms which play an important role during the early stages of the Universe evolution. However, the branching points take also place in models with $\bar{R}^{-1}$-type correction terms [19]. These terms play an important role at late times of the evolution of the Universe. Therefore, bouncing inflation may be responsible for the late-time accelerating expansion of the Universe.

To conclude our paper, we want to make a few comments. First, there is no need for fine tuning of the initial conditions to get the bouncing inflation. In Figs. 7–9, we have chosen for definiteness the initial conditions $\theta = 3.5$ and $E_{\text{kin}} = 0$. However, our calculations show that these figures do not qualitatively change if we take arbitrary $\theta \in (\pi, 2\pi)$ and nonzero E_{kin}. Second, Fig. 6 indicates that the minimum at $\theta = 2\pi$ is stable with respect to tunneling through the barrier at this point. The situation is similar to the quantum mechanical problem with infinitely high barrier. We have already stressed that the form of the potential Fig. 5 is not sufficient to predict the dynamical behavior of θ. This field has very nontrivial behavior because of the noncanonical kinetic term and singular (at the matching points) nonflat moduli space metric $G(\theta)$. Therefore, it is impossible to ''jump'' quantum mechanically from one branch to another. We cannot apply to our dynamical system the standard tunneling approach (e.g., in [27]). This problem needs a separate investigation. Third, it is worth noting that the Universe with a bounce preceding the inflationary period was considered in [28] where it was shown that due to a bounce, the spectrum of primordial perturbations has the characteristic features. It indicates that the similar effect can take place in our model. This is an interesting problem for future research.

ACKNOWLEDGMENTS

We want to thank Uwe Günther for useful comments. We also would like to thank Yi-Fu Cai for drawing our attention to their paper [28]. This work was supported in part by the ''Cosmomicrophysics'' programme of the Physics and Astronomy Division of the National Academy of Sciences of Ukraine.

APPENDIX: BOUNCING INFLATION IN THE BRANS-DICKE FRAME

According to Eq. (2.7), the four-dimensional Friedmann-Robertson-Walker metrics in the Einstein

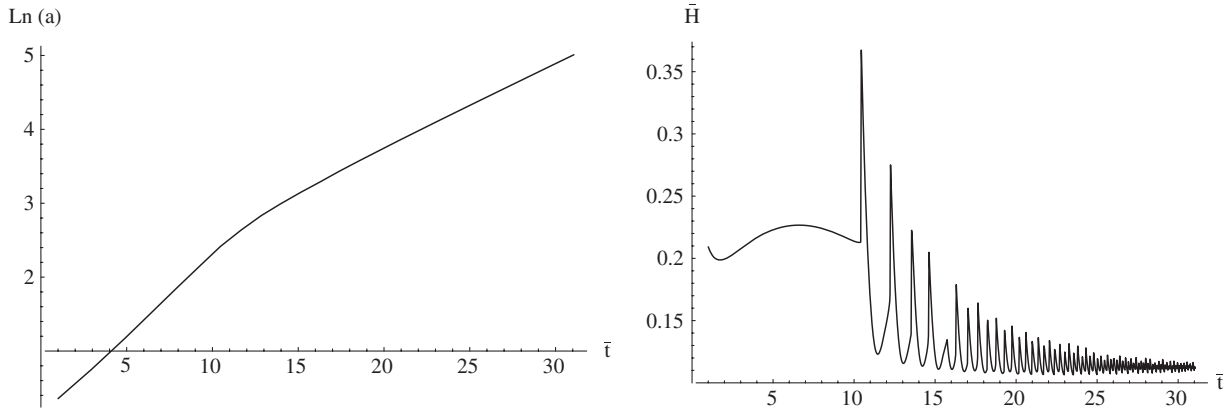

FIG. 13. The time evolution of the logarithms of the scale factor $\bar{a}(\bar{t})$ (left panel) and the Hubble parameter $\bar{H}(\bar{t})$ (right panel) for the trajectory drawn in Fig. 7 in the Brans-Dicke frame.

frame (5.1) and in the Brans-Dicke frame are related as follows:

$$-dt \otimes dt + a^2(t) d\vec{x} \otimes d\vec{x} = f'[-d\bar{t} \otimes d\bar{t} + \bar{a}^2(\bar{t}) d\vec{x} \otimes d\vec{x}], \tag{A1}$$

where $f' = X + 1 > 0$ and X is parametrized by Eq. (5.3). Therefore, for the synchronous times and scale factors in both frames we obtain, correspondingly,

$$d\bar{t} = dt/\sqrt{f'(t)}, \tag{A2}$$

$$\bar{a}(\bar{t}) = a(t(\bar{t}))/\sqrt{f'(t(\bar{t}))}, \tag{A3}$$

which lead to the following equations:

$$\bar{t} = \int_1^t \frac{dt}{\sqrt{X(t) + 1}} + 1, \tag{A4}$$

where we choose the constant of integration in such a way that $\bar{t}(t = 1) = 1$, and

$$\bar{H}(\bar{t}) = \frac{d\bar{a}}{d\bar{t}} \frac{1}{\bar{a}} = \sqrt{X(t(\bar{t})) + 1} \left[H(t(\bar{t})) - \frac{1}{2(X(t(\bar{t})) + 1)} \frac{dX}{dt}(t(\bar{t})) \right]. \tag{A5}$$

From the latter equation, we get the relation between the Hubble parameters in both frames. We plot in Fig. 13 the logarithms of the scale factor $\bar{a}(\bar{t})$ and the Hubble parameter $\bar{H}(\bar{t})$ for the trajectory drawn in Fig. 7. These pictures clearly demonstrate that in the Brans-Dicke frame the Universe also has an asymptotical de Sitter stage when the scalaron field approaches the branching point $\theta = 2\pi$. It is not difficult to verify that because $X(t \to +\infty) \to X_{\max}$ and $dX/dt(t \to +\infty) \to 0$; we obtain the following relation for the asymptotic values of the Hubble parameters in both frames:

$$\bar{H} = H\sqrt{X_{\max} + 1}. \tag{A6}$$

[1] A. A. Starobinsky, Phys. Lett. **91B**, 99 (1980).
[2] N. D. Birrell and P. C. W. Davies, *Quantum Fields in Curved Space* (Cambridge University Press, Cambridge, England, 1982).
[3] S. Nojiri and S. D. Odintsov, Phys. Lett. B **576**, 5 (2003).
[4] R. P. Woodard, Lect. Notes Phys. **720**, 403 (2007).
[5] S. Nojiri and S. D. Odintsov, Int. J. Geom. Methods Mod. Phys. **4**, 115 (2007); T. P. Sotiriou and V. Faraoni, Rev. Mod. Phys. **82**, 451 (2010).
[6] S. Capozziello, M. De Laurentis, and V. Faraoni, arXiv:0909.4672.
[7] B. Witt, Phys. Lett. **145B**, 176 (1984); V. Müller, H.-J. Schmidt, and A. A. Starobinsky, Phys. Lett. B **202**, 198 (1988); J. D. Barrow and S. Cotsakis, Phys. Lett. B **214**, 515 (1988).
[8] K.-I. Maeda, Phys. Rev. D **39**, 3159 (1989).
[9] S. Kaneda, S. V. Ketov, and N. Watanabe, arXiv:1001.5118; arXiv:1002.3659.
[10] U. Günther, A. Zhuk, V. B. Bezerra, and C. Romero, Classical Quantum Gravity **22**, 3135 (2005).
[11] T. Saidov and A. Zhuk, Phys. Rev. D **75**, 084037 (2007).
[12] S. M. Carroll, A. De Felice, V. Duvvuri, D. A. Easson, M. Trodden, and M. S. Turner, Phys. Rev. D **71**, 063513 (2005).
[13] J. Ellis, N. Kaloper, K. A. Olive, and J. Yokoyama, Phys. Rev. D **59**, 103503 (1999).

[14] U. Günther, P. Moniz, and A. Zhuk, Phys. Rev. D **66**, 044014 (2002).
[15] U. Günther, P. Moniz, and A. Zhuk, Phys. Rev. D **68**, 044010 (2003).
[16] T. Saidov and A. Zhuk, Gravitation Cosmol. **12**, 253 (2006).
[17] K. A. Bronnikov and S. G. Rubin, Gravitation Cosmol. **13**, 253 (2007).
[18] T. Saidov and A. Zhuk, Phys. Rev. D **79**, 024025 (2009).
[19] A. V. Frolov, Phys. Rev. Lett. **101**, 061103 (2008).
[20] U. Günther and A. Zhuk, *Proceedings of the Xth Marcel Grossmann Meeting on General Relativity "MG10" in Rio de Janeiro, Brazil, 2003*, edited by M. Novelo, S. P. Bergliaffa, and R. Ruffini (World Scientific, Singapore, 2006), p. 877.
[21] V. Faraoni, Phys. Rev. D **75**, 067302 (2007).
[22] A. D. Dolgov and M. Kawasaki, Phys. Lett. B **573**, 1 (2003).
[23] A. A. Starobinsky, JETP Lett. **86**, 157 (2007).
[24] U. Günther and A. Zhuk, Phys. Rev. D **56**, 6391 (1997); M. Rainer and A. Zhuk, Phys. Rev. D **54**, 6186 (1996); U. Günther, A. Starobinsky, and A. Zhuk, Phys. Rev. D **69**, 044003 (2004).
[25] U. Günther and A. Zhuk, Phys. Rev. D **61**, 124001 (2000).
[26] R. Kallosh and S. Prokushkin, arXiv:hep-th/0403060.
[27] S. Coleman and F. De Luccia, Phys. Rev. D **21**, 3305 (1980).
[28] Yi-Fu Cai, Tao-tao Qiu, Jun-Qing Xia, and Xinmin Zhang, Phys. Rev. D **79**, 021303 (2009).